Extrapolated high-order propagators for path integral Monte Carlo simulations

Robert E. Zillich,[1,a)] Johannes M. Mayrhofer,[1,b)] and Siu A. Chin[1,2]
[1]*Institut für Theoretische Physik, Johannes Kepler Universität Linz, A-4040 Linz, Austria*
[2]*Department of Physics, Texas A&M University, College Station, Texas 77843, USA*

(Received 17 July 2009; accepted 1 January 2010; published online 22 January 2010)

We present a new class of high-order imaginary time propagators for path integral Monte Carlo simulations that require no higher order derivatives of the potential nor explicit quadratures of Gaussian trajectories. Higher orders are achieved by an extrapolation of the primitive second-order propagator involving subtractions. By requiring all terms of the extrapolated propagator to have the same Gaussian trajectory, the subtraction only affects the potential part of the path integral. The resulting violation of positivity has surprisingly little effects on the accuracy of the algorithms at practical time steps. Thus in principle, arbitrarily high order algorithms can be devised for path integral Monte Carlo simulations. We verified the fourth, sixth, and eighth order convergences of these algorithms by solving for the ground state energy and pair distribution function of liquid ^{4}He, which is representative of a dense, and strongly interacting, quantum many-body system.
 [doi:10.1063/1.3297888]

I. INTRODUCTION

Many quantum Monte Carlo (QMC) techniques, such as path integral (ground state) Monte Carlo [PI(GS)MC] and diffusion Monte Carlo (DMC), rely on stochastic propagation of the Schrödinger equation in imaginary time. In all these methods, the probability distribution sampled is the matrix element, or the trace, of the imaginary time propagator

$$G(\tau) = \mathrm{e}^{-\tau H} = \mathrm{e}^{-\tau(T+V)}, \tag{1}$$

with Hamiltonian $H=T+V$ and kinetic and potential operators $T=(-\hbar^2/2m)\Sigma_i\nabla_i^2$ and $V=\Sigma_{i<j}v(r_{ij})$. Since $G(\tau)$ is generally unknown, τ is usually discretized into a sum of short time steps ϵ so that the full propagator $G(\epsilon)$ can be approximated by a product of short-time approximate propagator $\tilde{G}(\epsilon)$. If $\tilde{G}(\epsilon)$ is accurate to high orders in ϵ, then a large ϵ can be used to span a given imaginary time interval, resulting in fewer samplings of (but possibly computationally more complex) $\tilde{G}(\epsilon)$. As recently demonstrated by Sakkos, Casulleras, and Boronat,[1] such a higher order propagator can be highly efficient in projecting out ground state properties by minimizing the number of "beads," or time slices, required in large scale path integral Monte Carlo (PIMC) calculations. Hence, the ability to use large time steps is one way to improve efficiency. Other measures to improve efficiency are "smarter" MC sampling moves, as was impressively demonstrated by the worm algorithm for PIMC simulations at finite temperature.[2] The present work is about the first kind of efficiency improvement, "smarter" propagators.

For QMC simulations, there is a surprising lack of general higher order algorithms. For example, one has the well known second order, primitive propagator

$$G_2(\epsilon) = \mathrm{e}^{-\epsilon V/2}\mathrm{e}^{-\epsilon T}\mathrm{e}^{-\epsilon V/2} = G(\epsilon) + O(\epsilon^3). \tag{2}$$

(For computing the trace, any splitting first-order algorithm, such as $\mathrm{e}^{-\epsilon V}\mathrm{e}^{-\epsilon T}$, will also yield a second-order trace.[3]) The highly successful pair-density propagator, which approximates G by a pairwise product of exact two-body propagators,[4] must also be second order in the general many-particle case, but possibly with a very small error coefficient. (Reference 5 showed an empirical cubic convergence for a cluster of 22 hydrogen molecules. For such a small cluster, only 5 particles are in the core region of density $\rho \approx 0.02$ Å^{-3}. The remaining 17 particles are at the surface region with an average density of only 0.009 Å^{-3}. Since the pair-density propagator is exact in the low density limit, this excellent behavior is not unexpected. However, the off-diagonal pair density was later found not to be properly implemented.[6]) The necessity of evaluating the exact two-particle density matrix also limits the pair-density algorithm to only spherically symmetric interactions.

The only fourth-order method known for many years is the Takahashi–Imada,[7] Li–Broughton[8] propagator

$$G_{\mathrm{TI}}(\epsilon) = \mathrm{e}^{-\epsilon T/2}\mathrm{e}^{-\epsilon V-(\epsilon^3/24)[V,[T,V]]}\mathrm{e}^{-\epsilon T/2} = G(\epsilon) + O(\epsilon^3), \tag{3}$$

where $[V,[T,V]]=(\hbar^2/m)\Sigma_i|\nabla_i V|^2$. This "corrector" propagator is only second order, but yields a fourth-order trace, as explained in Ref. 3. Thus until recently, there were only two second-order and one fourth-order algorithm for PIMC simulations.

The problem of constructing higher order PIMC algorithms is the *time-irreversible* nature of the imaginary time Schrödinger equation. The short-time propagator can in gen-

a)Electronic mail: robert.zillich@jku.at.
b)Present address: Institut für Pharmakologie und Toxikologie, Universität Zürich, Switzerland.

eral be approximated to any order by a product decomposition,

$$e^{-\epsilon(T+V)} \approx \prod_{i=1}^{N} e^{-t_i \epsilon T} e^{-v_i \epsilon V}, \tag{4}$$

with coefficients $\{t_i, v_i\}$ determined by the required order of accuracy. However, in QMC applications, since $\langle R'|e^{-t_i \epsilon T}|R\rangle \propto e^{-(R'-R)^2/(4Dt_i\epsilon)}$ is the diffusion kernel with $D=\hbar^2/2m$, the coefficient t_i must be positive in order for the kernel to be normalizable as a probability distribution. As first proved by Sheng[9] and Suzuki,[10] and later by Goldman–Kaper[11] and Chin,[12] beyond second order, any factorization of the form (4) *must* contain some negative coefficients in the set $\{t_i, v_i\}$. Thus, despite myriad of higher-order propagators of the single product form (4) for solving the *time-reversible*, real-time Schrödinger equation, none can be applied in PIMC beyond second order. It is only in the last decade that bona fide fourth order, *forward* algorithms with all positive coefficients have been found[13,14] and applied to DMC and PIMC simulations.[15–17] In order to circumvent the Sheng–Suzuki theorem, one must include the operator $[V,[T,V]]$ in the factorization process. Unfortunately, it is not possible to go beyond fourth-order by including more operators. It has been shown[18] that a forward sixth-order propagator would have required the operator $[V,[T,[T,[T,V]]]]$, which is nonseparable and impractical to implement. Recently, by fine-tuning a family of fourth-order forward algorithm with two free parameters[19] such that the fourth-order error is zero, Sakkos, Casulleras and Boronat,[1] and later also one of us,[20] have achieved sixth-order convergence in computing the energy of a number of quantum systems including liquid ^{4}He. Despite this spectacular advance, it must be noted that the fine-tuning must be done, in principle, for each individual observable. The algorithm is therefore only "quasi" sixth-order rather than uniformly sixth-order.

There are recent attempts of deriving fourth and higher order PIMC algorithms without the use of operator splitting, which is the principle focus of this work. The algorithm derived by Bogojević *et al.*[21,22] required higher and higher order derivatives of the potential, which are increasingly singular for Lennard-Jones type potentials and difficult to implement for more than a few particles. Predescu[23,24] approximated the Feynman–Kac formula via a stochastic version of the Magnus expansion, requiring explicit quadrature of random trajectories and applicable only to potentials with finite Gaussian transforms. This excluded most Lennard-Jones type potentials with a strongly repulsive core. Both algorithms showed fourth-order convergence only for very smooth quartic, exponential, or sum of cosines potentials,[25] while for a one-dimensional Lennard-Jones model, convergence to fourth order seemed only asymptotic.[23] Both of these recent methods have yet to be fully tested on a strongly interacting, realistic many-body system.

In this paper, we will present the first QMC simulation using a bona fide sixth- and eighth-order algorithms. These algorithms use only the potential and have no need of explicit quadratures. They are based on the multi-product expansion[26] of the short time propagator, which is an alternative way of circumventing the Sheng–Suzuki Theorem in achieving higher order convergences. This is reviewed in Sec. II A and followed by a brief introduction to path integral ground state Monte Carlo (PIGSMC) in Sec. II B. Section III verifies the order of convergence of these extrapolated algorithms when solving for the ground state properties of bulk liquid helium using 64 particles. Liquid helium is a widely recognized, strongly interacting and very dense, quantum many-body system.

II. THEORY

A. Multi-product expansion of *G*

Let $G_2(\epsilon)$ denote the second-order split propagator (2), then for a given set of n whole numbers $\{k_i\}$, the multi-product expansion of Ref. 26 yields the following 2n-order propagator:

$$G_{2n}(\epsilon) = \sum_{i=1}^{n} c_i G_2^{k_i}(\epsilon/k_i) = G(\epsilon) + O(\epsilon^{2n+1}), \tag{5}$$

where the expansion coefficient has the closed form

$$c_i = \prod_{j=1(\neq i)}^{n} \frac{k_i^2}{k_i^2 - k_j^2}. \tag{6}$$

For PI(GS)MC, it is convenient to choose the sequences $\{k_i\}=\{1,2\}$, $\{1,2,4\}$ and $\{1,2,3,6\}$ to produce the following fourth, sixth, and eighth-order propagators:

$$G_4(\epsilon) = -\frac{1}{3}G_2(\epsilon) + \frac{4}{3}G_2^2\left(\frac{\epsilon}{2}\right), \tag{7}$$

$$G_6(\epsilon) = \frac{1}{45}G_2(\epsilon) - \frac{4}{9}G_2^2\left(\frac{\epsilon}{2}\right) + \frac{64}{45}G_2^4\left(\frac{\epsilon}{4}\right), \tag{8}$$

$$G_8(\epsilon) = -\frac{1}{840}G_2(\epsilon) + \frac{2}{15}G_2^2\left(\frac{\epsilon}{2}\right) - \frac{27}{40}G_2^3\left(\frac{\epsilon}{3}\right) + \frac{54}{35}G_2^6\left(\frac{\epsilon}{6}\right). \tag{9}$$

As we will see later, these sequences are chosen because they are the minimal "commensurate" sequences. Schmidt and Lee[27] previously suggested the use of Eq. (7) in path integrals and did use it in computing the two-particle density matrix. However, they did not suggest that it can be used for doing PIMCs. Brualla[28] suggested extrapolations not of the propagator, but of the energy using reweighting which, however, lead to large statistical noise.

Since $G(\epsilon)>0$, only the error terms in Eq. (5) can be negative. Thus for sufficiently small ϵ, these extrapolated propagators, despite the explicit subtractions, are mostly positive. Only when ϵ is very large can the error terms overwhelm $G(\epsilon)$ in a significant fraction of the configuration space. However, such large ϵ cannot be used anyway because the propagators would then be highly inaccurate. One might argue that the error terms can be so singular that despite the smallness of ϵ, it can overwhelm $G(\epsilon)$ at some specific locations. However, this cannot happen because by construction

$G_2(\epsilon)$ is bounded everywhere and the subtraction of two bounded functions cannot be singular. As we will see below, the subtraction is further limited to subtracting only exponentials of the potential energy, and each exponential is everywhere bounded for Lennard-Jones type potentials with a repulsive core. The exception is the attractive Coulomb potential, for which $G_2(\epsilon)$ is singular at the origin and its use in naive PIMC simulation does not give the expected quadratic convergence. However, as shown by Li and Broughton,[8] quadratic convergence can be restored by implementing the Takahashi–Imada[7] propagator, which is everywhere nonsingular at a finite ϵ. (Note that the commutation $[V,[T,V]]$ is part of the propagator only and should *not* be included in computing the energy.) In this work, we will assume that we are extrapolating a $G_2(\epsilon)$ that is quadratically convergent. For the Coulomb potential, one must not use the naive $G_2(\epsilon)$ of Eq. (2), but replace it with $G_{TI}(\epsilon)$ of Eq. (3) instead.

B. Path integral ground state Monte Carlo

The above multiproduct propagators can be applied to any general PIMC simulations. Here, we will implement it in the specific context of PIGSMC. PIGSMC samples the whole probability distribution function corresponding to a discretized imaginary time propagation from a trial wave function $\Psi_T(R)$ to the (in principle) exact ground state $\Psi_0(R)$, where R denotes all degrees of freedom, e.g., for the translational coordinates of N particles, $R=(\mathbf{r}_1,\ldots,\mathbf{r}_N)$.

For any trial wave function Ψ_T with nonzero overlap with the exact ground state, the exact ground state wave function can be obtained by evolving in imaginary time

$$\Psi_0(R) \propto \lim_{\beta/2\to\infty} \int G\left(R,R',\frac{\beta}{2}\right)\Psi_T(R')dR'.$$

$G(\beta/2)$ is evaluated by factorizing it into a product of small time step propagators $G(\epsilon)$, $\epsilon=\beta/2M$, which can be approximate by one of the above-mentioned short time approximations. Therefore, the full probability distribution to be sampled is

$$P(R_0,\ldots,R_{2M}) = \frac{1}{\mathcal{N}}\Psi_T(R_0)G(R_0,R_1;\epsilon)\ldots G(R_{2M-1},R_{2M};\epsilon)\Psi_T(R_{2M}),$$

so that the expectation value $\langle\Psi_0|A|\Psi_0\rangle$ of a local operator $A(R)$ is evaluated by sampling A at the central time step, $A(R_M)$. For the energy, we take advantage of $[H,G]=0$ to obtain the energy estimator in terms of the local energy of the trial wave function $E_L(R)=H\Psi_T/\Psi_T$,

$$E_0 = \int dR_0\ldots dR_{2M}E_L(R_0)P(R_0,\ldots,R_{2M}).$$

These multi-dimensional integrations can be carried out with the Metropolis method.

C. Implementing multi-product expansions in PIGSMC

To see how one can implement these multi-product propagators in PIGSMC, we will now give a detailed discussion of the fourth order case. Considering G_4 at time step size 2ϵ,

$$G_4(2\epsilon) = \tfrac{4}{3}e^{-\epsilon V/2}e^{-\epsilon T}e^{-\epsilon V}e^{-\epsilon T}e^{-\epsilon V/2} - \tfrac{1}{3}e^{-\epsilon V}e^{-2\epsilon T}e^{-\epsilon V}.$$

In evaluating the matrix element of $G_4(2\epsilon)$, since the first term on the right hand side has one more operator $e^{-\epsilon T}$, it would require one more intermediate state integration than the second term, resulting in two dissimilar terms difficult to sample uniformly. That is, each term corresponds to sampling a different Gaussian random path with a different variance. One of the key contribution of this work is to enforce uniformity by artificially splitting the single operator $e^{-2\epsilon T}$ in the second term into two,

$$G_4(2\epsilon) = \tfrac{4}{3}e^{-\epsilon V/2}e^{-\epsilon T}e^{-\epsilon V}e^{-\epsilon T}e^{-\epsilon V/2} - \tfrac{1}{3}e^{-\epsilon V}e^{-\epsilon T}e^{-\epsilon T}e^{-\epsilon V}, \tag{10}$$

which then results in the following coordinate representation:

$$\begin{aligned}\langle 1|G_4(2\epsilon)|3\rangle &= \int d2\langle 1|e^{-\epsilon T}|2\rangle\langle 2|e^{-\epsilon T}|3\rangle \\ &\quad\times\left[\frac{4}{3}e^{-\epsilon V_1/2-\epsilon V_2-\epsilon V_3/2} - \frac{1}{3}e^{-\epsilon V_1-\epsilon V_3}\right] \\ &= \int d2G_0(12;\epsilon)G_0(23;\epsilon) \\ &\quad\times e^{-\epsilon V_1/2-\epsilon V_2-\epsilon V_3/2}F(123,\epsilon),\end{aligned} \tag{11}$$

where we have abbreviated $V_k=V(R_k)$, $R_k\to k$ and denoted

$$F(123,\epsilon) = \tfrac{1}{3}[4 - e^{-\epsilon(V_1+V_3)/2-\epsilon V_2}], \tag{12}$$

and the free propagator

$$G_0(12;\epsilon) = \langle 1|e^{-\epsilon T}|2\rangle = (4\pi D\epsilon)^{-3N/2}e^{-(R_1-R_2)^2/4D\epsilon}. \tag{13}$$

We observe that (1) without the factor F, Eq. (11) is just the second-order algorithm repeated twice. (2) By including F, only the potential energy needs to be extrapolated to achieve fourth-order accuracy. (3) For sufficiently small ϵ, $F>0$. (4) If the potential function is mostly convex (such as Lennard-Jones type potential near the potential minimum), then one has

$$\frac{V(R_1)+V(R_3)}{2} \geq V\left(\frac{R_1+R_3}{2}\right). \tag{14}$$

Since

$$G_0(12;\epsilon)G_0(23;\epsilon) = \frac{e^{-(1/2D\epsilon)(R_2-(R_1+R_3)/2)^2}}{(2\pi D\epsilon)^{3N/2}}G_0(13;2\epsilon),$$

for fixed R_1 and R_3, R_2 is normally distributed about $(R_1+R_3)/2$ with width $\propto\sqrt{\epsilon}$. If R_2 is such that it is between R_1 and R_3, then the convexity condition (14) would guarantee Eq. (12) to be positive for all ϵ. This only fails when the width of the Gaussian distribution for R_2 exceeds $|R_1-R_3|/2$, suggesting that the near-positivity of F can extend over a rather wide range of ϵ, which is indeed observed.

Metropolis sampling requires exact positivity of F, which we ensure by using $\max(0,F)$, i.e., rejecting moves where $F<0$. We also collect statistics about these rejections, to ensure that their rate is low, and decreasing with ϵ.

For a system of particles subject to an external potential V_{ext}, in addition to the interaction potential, V_{ext} could be incorporated in G_0 rather than in the potential V_i. G_0 becomes a product of the exact single-particle propagators, and the potential V_i in Eq. (12) is still the pure interaction potential. In particular, G_4 is then separable in the sense that, for noninteracting particles, G_4 is just the product of single-particle propagators G_0.

The generalization to higher order is now clear. For the sixth-order, Eq. (8),

$$G_6(4\epsilon) = \frac{64}{45}e^{-\epsilon V/2}e^{-\epsilon T}e^{-\epsilon V}e^{-\epsilon T}e^{-\epsilon V}e^{-\epsilon T}e^{-\epsilon V}e^{-\epsilon T}e^{-\epsilon V/2} - \frac{4}{9}e^{-\epsilon V}e^{-\epsilon T}e^{-\epsilon T}e^{-2\epsilon V}e^{-\epsilon T}e^{-\epsilon T}e^{-\epsilon V} + \frac{1}{45}e^{-2\epsilon V}e^{-\epsilon T}e^{-\epsilon T}e^{-\epsilon T}e^{-\epsilon T}e^{-2\epsilon V}, \quad (15)$$

yielding the coordinate representation

$$G_6(12345;4\epsilon) = G_0(12;\epsilon)G_0(23;\epsilon)G_0(34;\epsilon)G_0(45;\epsilon) \times \left[\frac{64}{45}e^{-\epsilon V_1/2-\epsilon V_2-\epsilon V_3-\epsilon V_4-\epsilon V_5/2} - \frac{4}{9}e^{-\epsilon V_1-2\epsilon V_3-\epsilon V_5} + \frac{1}{45}e^{-2\epsilon V_1-2\epsilon V_5}\right]. \quad (16)$$

Similarly for the eighth-order Eq. (9),

$$G_8(1234567;6\epsilon) = G_0(12;\epsilon)G_0(23;\epsilon)\ldots G_0(67;\epsilon) \times \left[\frac{54}{35}e^{-\epsilon V_1/2}e^{-\epsilon V_2}e^{-\epsilon V_3}e^{-\epsilon V_4}e^{-\epsilon V_5}e^{-\epsilon V_6}e^{-\epsilon V_7/2} - \frac{27}{40}e^{-\epsilon V_1}e^{-2\epsilon V_3}e^{-2\epsilon V_5}e^{-\epsilon V_7} + \frac{2}{15}e^{-3\epsilon V_1/2}e^{-3\epsilon V_4}e^{-3\epsilon V_7/2} - \frac{1}{840}e^{-3\epsilon V_1}e^{-3\epsilon V_7}\right]. \quad (17)$$

For commensurate sequences one can factor out all the free-propagators and restrict the extrapolation process only to the potential energy function.

III. RESULTS

We have implemented the PIGSMC algorithm using multilevel sampling as described in the review Ref. 4 We compare our new extrapolated fourth, sixth, and eighth order propagators with the primitive (second-order) and the fourth-order forward propagators[14] 4A,

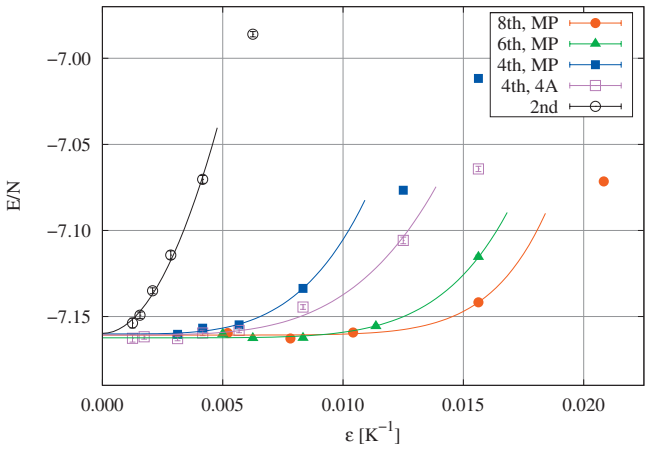

FIG. 1. Ground state energy E_0 of bulk ^{4}He, simulated by 64 ^{4}He atoms, as a function of imaginary time step ϵ. Decay time was $\beta=0.25$ K^{-1}. We compare results produced by the primitive second-order propagator $G_2(\epsilon)$ and the fourth-order forward propagator (Ref. 14) $G_{4A}(\epsilon)$ (denoted "4A") with our fourth, sixth, and eighth-order multiproduct propagators $G_4(\epsilon)$, $G_6(\epsilon)$, and $G_8(\epsilon)$, (denoted "MP"). Each $E_0(\epsilon)$ is fitted with the appropriate polynomial.

$$G_{4A}(\epsilon) = e^{-(\epsilon/6)V}e^{-(\epsilon/2)T}e^{-(2\epsilon/3)V-(\epsilon^3/72)[V,[T,V]]}e^{-(\epsilon/2)T}e^{-(\epsilon/6)V}. \quad (18)$$

To demonstrate that our multi-product propagators work for realistic, and strongly interacting quantum systems, we apply them to the case of bulk liquid ^{4}He. We calculate the ground state energy E_0 at equilibrium density $\rho_0 = 0.021\,86$ Å^{-3}, by a PIGSMC simulation of 64 ^{4}He atoms in a simulation box with periodic boundary conditions. The decay time is $\beta=0.25$ K^{-1}, and we use the potential by Aziz *et al.*[29] In Fig. 1 we show E_0/N as function of ϵ for various propagators. We fit the polynomial $a+b\epsilon^n$ (lines) to $E_0(\epsilon)/N$, where n is the order of the respective propagator. Since the order of $E_0(\epsilon)$ is defined as the $\epsilon\to 0$ behavior, we have restricted the fits to small values of ϵ—the end point of the lines indicate the fitting interval. These propagators are compared at equal time steps: $G_2(\epsilon)$, $G_4(\epsilon)$, $G_6(\epsilon)$, and $G_8(\epsilon)$, to verify the order of convergence.

The primitive second-order propagator (open circle) is clearly a poor approximation, with a large error even for small ϵ, and therefore requires a large number of beads. The simplest fourth-order forward propagator 4A, Eq. (18), is a significant improvement, as can be seen in the behavior of $E_0(\epsilon)/N$ (open square), with error coefficient smaller than our fourth-order multiproduct propagator (11) (filled square). However, the forward 4A propagator requires the computation of $[V,[T,V]] \propto |\nabla_i V|^2$, and its relative efficiency would depend on the complexity of evaluating this gradient. Both can be fitted well by a fourth-order polynomial with $n=4$. Finally, the closed triangles and circles show the convergence of the sixth order Eq. (16) and eighth order Eq. (17) multiproduct expansion, which indeed has a smaller ϵ dependence in the range of Fig. 1. These multi-product propagators are true high order propagators and will produce sixth and eighth order convergences for the expectation value of any observable. The present results constitute the first implementation of a QMC simulation with a bona fide imaginary time

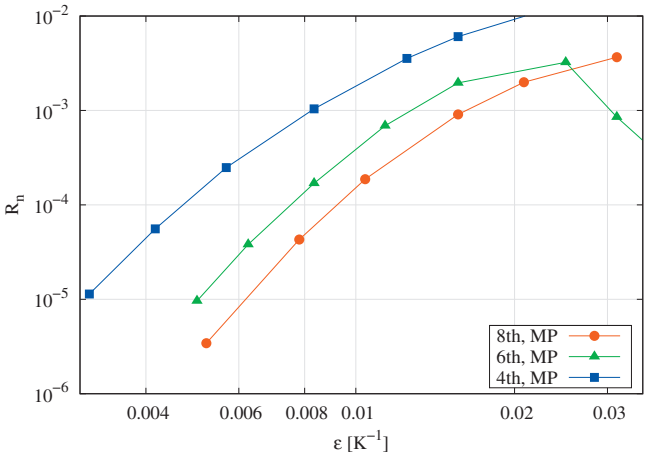

FIG. 2. The ratio R_n of rejected MC moves that would lead to a negative propagator G. R_n is decreasing with time step ϵ.

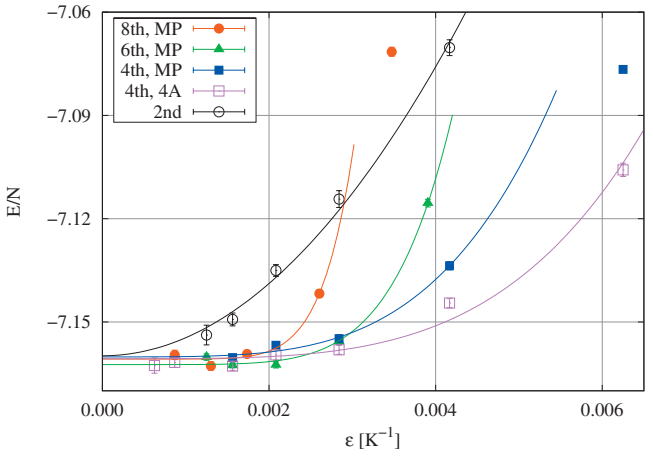

FIG. 3. A roughly equal effort comparison of algorithms $G_2(\epsilon)$, $G_4(2\epsilon)$, $G_6(4\epsilon)$, $G_8(6\epsilon)$, and $G_{4A}(2\epsilon)$ for the same ground state energy E_0 as in Fig. 1.

propagator of higher than fourth order. At small values of the time step size, say at ϵ=0.005, the sixth and eighth order algorithms produce very precise results, which are not indicated by Fig. 1.

The multi-product expansion of G, Eq. (5), is not strictly positive everywhere for a finite time step ϵ, as we have discussed above for the fourth-order case. In Fig. 2 we show the ratio R_n of attempted MC moves that are rejected due to negativity of the multiproduct expansion. R_n is decreasing with ϵ as expected. Only in the sixth-order case we observed a nonmonotonous behavior at very large ϵ where the ratio R_n *decreases* with increasing ϵ. This occurs at large values of ϵ where the error of the energy $E_0(\epsilon)/N$ is rapidly increasing with ϵ (outside the range of Fig. 1). This may due to system configurations with complicated intertwining negative and positive regions of G. We want to stress that, since this happens only for ϵ much too large for quantitatively correct results, it poses no practical limitations.

The convergence plot Fig. 1 does not reveal the actual computational effort required for a desired accuracy. From our derivation, it is clear that the computational effort of G_4, G_6, and G_8 are roughly equivalent to running G_2 twice, four, and six times, respectively. This then means that for a given ϵ for $G_2(\epsilon)$, one should compare it to G_4 at 2ϵ, G_6 at 4ϵ, and G_8 at 6ϵ, that is, for an equal effort comparison, we should compare $G_2(\epsilon)$, $G_4(2\epsilon)$, $G_6(4\epsilon)$, and $G_8(6\epsilon)$. This is done in Fig. 3. In this comparison, at a given ϵ each algorithm uses the same number of beads. For the forward algorithm 4A, this comparison neglects the additional cost of evaluating the gradient $|\nabla_i V|^2$. If $|\nabla_i V|^2$ required no additional effort to that of evaluating the potential, then propagator 4A would actually outperform the extrapolated sixth- and eighth-order algorithms at time steps $\epsilon \gtrsim 0.003$ K^{-1}. This confirms that, in principle, a purely forward time step algorithm can be more efficient, provided that $|\nabla_i V|^2$ can be easily evaluated. However, the higher order extrapolated algorithms are clearly easier to derive and implement. Moreover, when very high accuracy is required, such as the "chemical accuracy" required in quantum chemistry applications, then a higher order algorithm will always outperform a lower order algorithm. This is especially critical in determining the equilibrium configuration or conformation of clusters and macromolecules, where energy differences are very small. Another example where high accuracy is required is the study of quantum phase transitions, such as solidification of a ^{4}He layer on graphene.[30]

The ground state energy E_0 is of course not the only expectation value of interest that can be evaluated by QMC simulations. An important structural quantity is the pair distribution function $g(r)$, the probability density for two particles separated by a distance r, normalized to $g(r\to\infty)=1$. For bulk systems, $g(r)$ can be measured, and thus provides another possibility to assess the accuracy of the interaction potential model by comparing QMC and experimental results for $g(r)$. However the calculation of such structural quantities by QMC is crucial if they cannot be obtained experimentally. For example, in helium nanodroplet isolation spectroscopy where chromophores are embedded in ^{4}He droplets, determining the chromophore-helium pair distribution function is essential for the calculation of absorption spectra.[31]

The time step-size error in observables other than E_0 is rarely examined in the literature. Here, we verify that our algorithms are truly higher orders by showing the convergence of the pair-distribution $g(r)$ of bulk liquid helium. We compute $g(r)$ by taking averages from configurations at the central time step, R_M, and binning the distances of all pairs of particles with bin size Δr=0.18 Å. We examine the convergence of $g(r)$ at four different distances r_i: at a small distance r_1=2.06 Å, almost inside the correlation hole, where $g(r)$ is strongly suppressed due to the repulsive part of the He–He interaction; at r_2=2.77 Å, where $g(r)$ is steep and rising to the maximum; at r_3=3.48 Å, where $g(r)$ attains its maximum (within the bin size); and at r_4=4.38 Å, between the maximum and the first local minimum of $g(r)$. In the four panels of Fig. 4 we show the pair distribution function $g(r_i;\epsilon)$ as a function of the imaginary time step ϵ. In each panel, we indicate the location of r_i by arrows in insets showing $g(r)$. We compare our results obtained by the fourth-order forward propagator[14] $G_{4A}(\epsilon)$ with our fourth, sixth, and eighth-order multiproduct propagators $G_4(\epsilon)$,

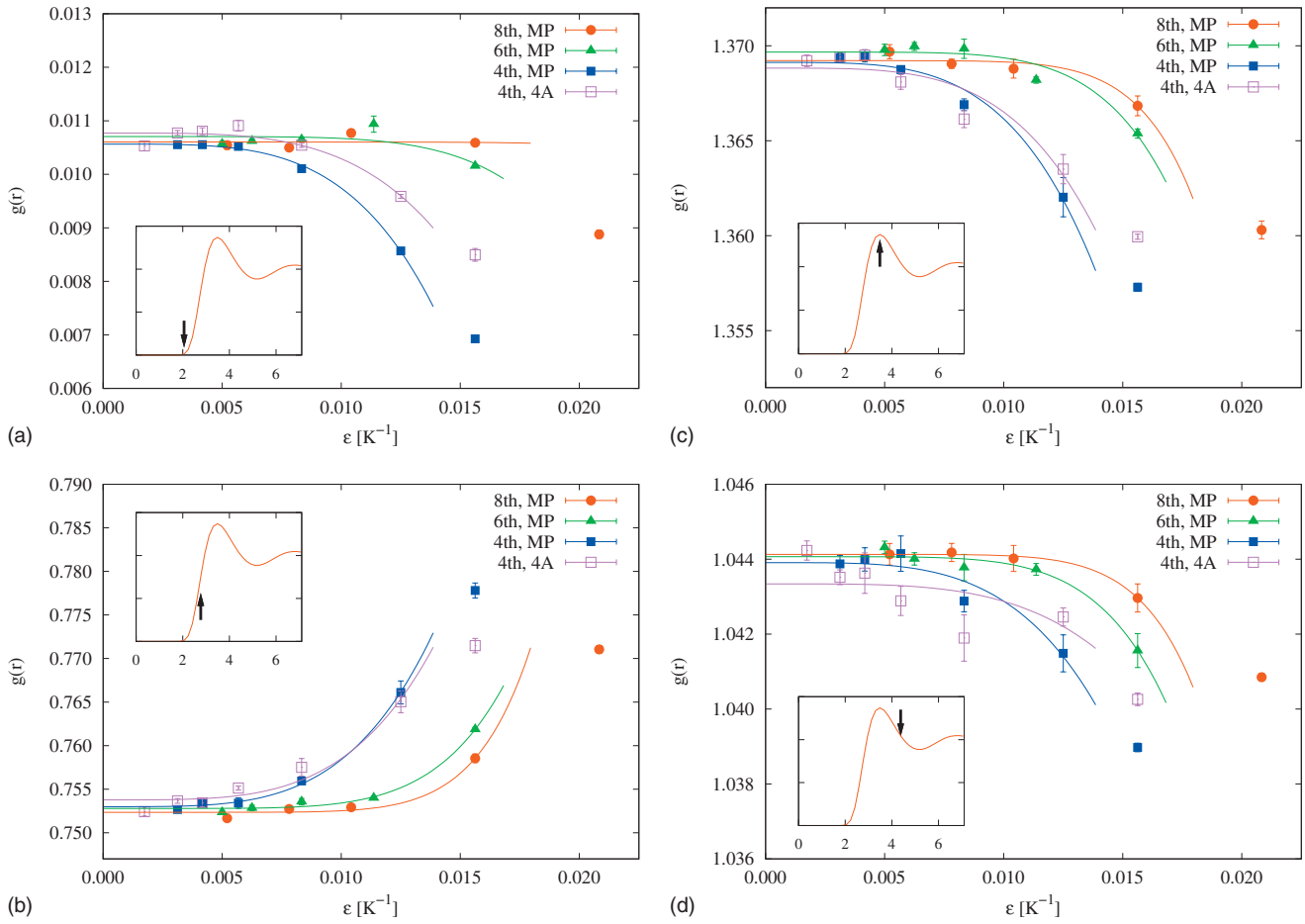

FIG. 4. The pair distribution function $g(r)$ of bulk ^{4}He is shown as a function of the imaginary time step ϵ for four different values of r (indicated by arrows in the respective insets). We compare results produced by the fourth-order forward propagator (Ref. 14) $G_{4A}(\epsilon)$ (denoted "4A") with our fourth, sixth, and eighth-order multiproduct propagators $G_4(\epsilon)$, $G_6(\epsilon)$, and $G_8(\epsilon)$, (denoted "MP"). Each $g(r;\epsilon)$ is fitted with the appropriate polynomial in ϵ.

$G_6(\epsilon)$, and $G_8(\epsilon)$ [we omit results for $G_2(\epsilon)$ for clarity]. Each $g(r_i;\epsilon)$ is fitted by the appropriate polynomial in ϵ.

At all examined locations r_i, Fig. 4 shows that the convergence behavior of $g(r)$ is similar to that E_0, as befitting bona fide higher algorithms. The fourth order propagator G_{4A} and our multiproduct propagator $G_4(\epsilon)$ perform similarly well. The time step error is decreasing when we increase the order of the propagator to sixth order, and further to eighth order, as it should be. This demonstrates that the multiproduct propagators Eqs. (7)–(9)—and surely also propagators of higher than eighth order—are fully capable of producing correspondingly higher order convergence results, not just for the ground state energy $E_0=\langle H\rangle$ but also for general observables that do not commute with H. As in the case of E_0, the calculation of $g(r)$ is not adversely affected by the fact that multiproduct propagators are not strictly positive everywhere.

The time step dependence of $g(r_i;\epsilon)$ exhibits some trends that are valid for all propagators. On an absolute scale, the time step error is smallest for r_1, where $g(r)$ has a value of only about 1% of the asymptotic limit $g(r\to\infty)=1$. On a relative scale, however, the time step error becomes as large as about 30% in the top left panel of Fig. 4. We found the largest error not for r_3, where $g(r)$ attains its maximum, but for r_2, where the *derivative* of $g(r)$ attains its maximum. The steep "wall" of the correlation hole is clearly most susceptible to time step error. Finally, beyond the maximum of $g(r)$ at r_3, the error decreases rapidly as evidenced by the results for r_4 in the bottom right panel of Fig. 4—despite the relatively large derivative of $g(r)$ at r_4.

IV. CONCLUSION AND OUTLOOK

In this work, we have shown how to implement the multiproduct expansion of the imaginary time propagator in QMC for solving strongly interacting quantum many-body systems, such as ^{4}He, to any desired order in the imaginary time step ϵ. In particular this work is the first demonstration of truly sixth- and eighth-order QMC algorithms. In the case of ^{4}He, our results suggest that these higher than fourth-order algorithms may not be more efficient than purely forward time step fourth-order algorithms, but they do have the simplicity of not requiring the potential gradient. This is particularly useful in simulating non-Cartesian coordinate systems, such as molecules[32] with anisotropic constituents and rotational degrees of freedom. Moreover, these extrapolated propagators are the only higher order algorithms possible in cases where the double-commutator cannot be evaluated, such as for the diatoms-in-molecule potential.[33] Finally, for QMC applications where chemical accuracy is required, such as in determining equilibrium configurations and conforma-

tions, our sixth and higher order multiproduct propagators will be computationally more efficient than fourth-order propagators.

ACKNOWLEDGMENTS

We are grateful for helpful discussions with Eckhard Krotscheck and Joaquim Casulleras. The work was supported by the Austrian Science Fund FWF, Project No. P21924.

[1] K. Sakkos, J. Casulleras, and J. Boronat, J. Chem. Phys. **130**, 204109 (2009).
[2] M. Boninsegni, N. V. Prokof'ev, and B. V. Svistunov, Phys. Rev. E **74**, 036701 (2006).
[3] S. A. Chin, Phys. Rev. E **69**, 046118 (2004).
[4] D. M. Ceperley, Rev. Mod. Phys. **67**, 279 (1995).
[5] C. Chakravarty, M. C. Gordillo, and D. M. Ceperly, J. Chem. Phys. **109**, 2123 (1998).
[6] C. Predescu, D. Sabo, J. D. Doll, and D. L. Freeman, J. Chem. Phys. **119**, 2123 (2003).
[7] M. Takahashi and M. Imada, J. Phys. Soc. Jpn. **53**, 3765 (1984).
[8] X.-P. Li and J. Q. Broughton, J. Chem. Phys. **86**, 5094 (1987).
[9] Q. Sheng, IMA J. Numer. Anal. **9**, 199 (1989).
[10] M. Suzuki, J. Math. Phys. **32**, 400 (1991).
[11] D. Goldman and T. J. Kaper, SIAM (Soc. Ind. Appl. Math.) J. Numer. Anal. **33**, 349 (1996).
[12] S. A. Chin, Phys. Lett. A **354**, 373 (2006).
[13] M. Suzuki, in *Computer Simulation Studies in Condensed Matter Physics VIII*, edited by D. Landau, K. Mon, and H. Shuttler (Springer, Berlin, 1996).
[14] S. A. Chin, Phys. Lett. A **226**, 344 (1997).
[15] H. A. Forbert and S. A. Chin, Phys. Rev. E **63**, 016703 (2000).
[16] H. A. Forbert and S. A. Chin, Phys. Rev. B **63**, 144518 (2001).
[17] S. Jang, S. Jang, and G. A. Voth, J. Chem. Phys. **115**, 7832 (2001).
[18] S. A. Chin, Phys. Rev. E **71**, 016703 (2005).
[19] S. A. Chin and C. R. Chen, J. Chem. Phys. **117**, 1409 (2002).
[20] J. Mayrhofer, Master's thesis, Johannes Kepler University, Linz, 2008.
[21] A. Bogojević, A. Balaz, and A. Belić, Phys. Rev. Lett. **94**, 180403 (2005).
[22] A. Bogojević, I. Vidanovic, A. Balaz, and A. Belić, Phys. Lett. A **372**, 3341 (2008).
[23] C. Predescu, Phys. Rev. E **69**, 056701 (2004).
[24] C. Predescu, J. Phys. Chem. B **110**, 667 (2006).
[25] S. Chempath, C. Predescu, and A. T. Bell, J. Chem. Phys. **124**, 234101 (2006).
[26] S. A. Chin, e-print arXiv:0809.0914v2.
[27] K. E. Schmidt and M. A. Lee, Phys. Rev. E **51**, 5495 (1995).
[28] L. Brualla, Ph.D. thesis, Universitat Politecnica de Catalunya, 2002.
[29] R. A. Aziz, V. P. S. Nain, J. S. Carley, W. L. Taylor, and G. T. McConville, J. Phys. Chem. **70**, 4330 (1979).
[30] M. C. Gordillo and J. Boronat, Phys. Rev. Lett. **102**, 085303 (2009).
[31] R. E. Zillich, Y. Kwon, and K. B. Whaley, Phys. Rev. Lett. **93**, 250401 (2004).
[32] R. E. Zillich, F. Paesani, Y. Kwon, and K. B. Whaley, J. Chem. Phys. **123**, 114301 (2005).
[33] M. Leino, A. Viel, and R. E. Zillich, J. Chem. Phys. **129**, 184308 (2008).